Revised Manuscript of C002908D

Palladium(II) and platinum(II) complexes bearing κ^3SCS pincer ligand with azulene unit

Junpei Kuwabara, Goro Munezawa, Ken Okamoto, Takaki Kanbara*

Tsukuba Research Center for Interdisciplinary Materials Science (TIMS), Graduate School of Pure and Applied Sciences, University of Tsukuba, 1-1-1, Tennodai, Tsukuba 305-8573, Japan

Summary

Novel Pd and Pt SCS-pincer complexes with an azulene unit were synthesized from the reaction of a metal precursor with an azulene molecule having two thioamide moieties. The crystal structures of the complexes were confirmed by X-ray diffractional study. Their structural and optical properties were investigated in comparison with those of related complexes with a benzene and pyrrole unit by NMR and UV/Vis spectroscopy. DFT calculations for the azulene complexes revealed that the origin of the long-wavelength absorption is assigned to a transition from the metal center to the extended π system of the azulene unit.

Keywords: Azulene / Palladium / Pincer complex / Thioamide

Introduction

Pincer complexes of group 10 metals have been intensively investigated in the fields of catalysis and material science.[1] Pincer complexes generally have a tridentate ligand (ECE ligand) composed of a cyclometallating carbon and donating groups such as PR_2, NR_2 and SR. We have investigated pincer complexes bearing thioamide moieties as a donating group.[2-4] The strong interaction between the thioamide group and transition

metals allows the formation of stable SCS-pincer complexes with a central benzene unit from a reaction under mild conditions (**A** in Scheme 1). The flexible structure and strong coordination of the thioamide moiety in the pincer ligand make it possible to obtain SNS-pincer complexes with a central pyrrole unit[5] (**B** in Scheme 1), which is unstable in the case of another donating group because the five-membered pyrrole unit destabilizes the chelating M-E bond owing to steric strain.[6] The high capability of the thioamide-based ligand motivated us to synthesize a new pincer ligand with an azulene unit, which affords an SCS-pincer complex with a five-membered central unit (**C** in Scheme 1).

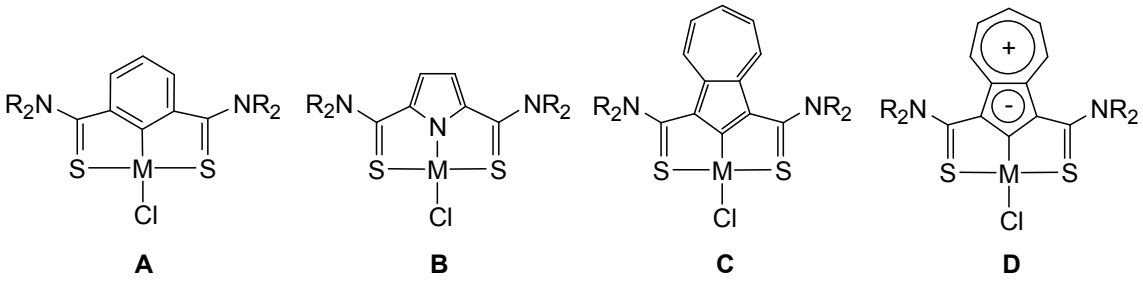

Scheme 1. Molecular structures of the M-(κ^3*SCS*) and M-(κ^3*SNS*) complexes.

Azulene is a nonbenzenoid aromatic compound consisting of a cyclopentadiene ring fused with a cycloheptatriene ring, which exhibits a blue color owing to the unique π-electron system. Azulene derivatives are utilized in the fields of optical materials,[7] conducting polymers[8] and colorimetric sensors of small molecules.[9] From the viewpoint of organometallic chemistry, azulene derivatives are recognized as conjugated π-ligands, which allow several coordination modes such as η^3 and η^5.[10] In contrast, there are limited examples of a single bond existing between a transition metal and a carbon atom in an azulene moiety owing to the large number of π-electrons having coordinative ability. Lash *et al.* reported Ni(II), Pd(II) and Pt(II) complexes with porphyrin derivatives incorporating an azulene unit (azuliporphyrins), which have a single bond between the transition metal and the azulene.[11] However, there is no example of a pincer

complex with an azulene unit to the best of our knowledge. Since one of the resonance structures of azulene can be described as a fused ring of a cyclopentadienyl anion and a cycloheptatrienyl cation (**D** in Scheme 1), the pincer complex is expected to undergo an interesting interaction between the electron-rich cyclopentadienyl anion moiety and the metal center through the carbon-metal bond and through the thioamide moiety. We here report the syntheses and crystal structures of the pincer complexes with the azulene unit as well as their optical properties. DFT calculations were performed to analyze the optical properties.

Results and discussion

Synthesis and NMR study

The pincer ligand with thioamide groups **1** was synthesized by the reaction of the corresponding amide molecule[12] with Lawesson's reagent.[13] The reaction of ligand **1** with $PdCl_2$ and LiCl in methanol at the reflux temperature yielded palladium-κ^3*SCS* pincer complex **2** with a 77% yield (Scheme 2). Similarly, Pt complex **3** was obtained with an 85% yield from the reaction of **1** with $PtCl_2(PhCN)_2$ in acetonitrile at 65 °C. Referenced compounds **4** and **5** were synthesized by a method similar to that previously reported. [5]

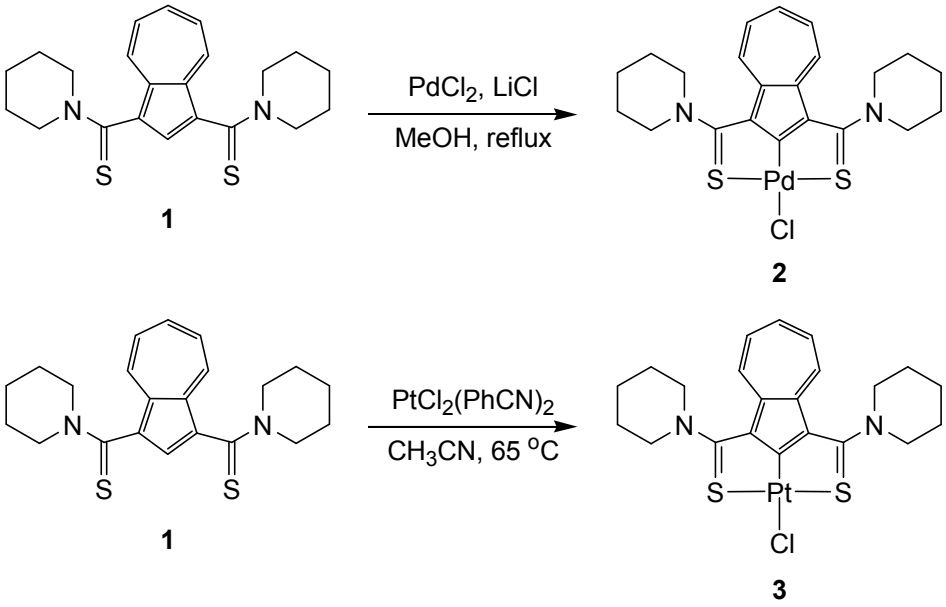

Scheme 2. Syntheses of the pincer Pd and Pt complexes with an azulene unit.

Compounds **1**-**3** were characterized by ^{1}H NMR, IR, mass spectroscopy and elemental analysis. The resonance of the C-H proton between the thioamide groups in ligand **1** (7.47 ppm) disappeared in the spectra of **2** and **3**, which proves the C-H bond activation at this position. In the ^{1}H NMR spectrum of **1**, the resonance of a -CH_2NCH_2- moiety in the piperidyl group appears nonequivalently at 4.47 and 2.78 ppm. The nonequivalence is probably due to the slow rotation of the piperidyl group owing to the contribution of the C=N double-bond character in the thioamide group, which is caused by the charge transfer from the N atom to the S atom as described in the literature (**E** in Scheme 3).[14] However, in the case of complexes **2** and **3**, the corresponding methylene resonance equivalently appears as a slightly broad resonance at 4.13 ppm for **2** and 4.14 ppm for **3**. These results indicate the small contribution of the C=N double-bond character in the pincer complexes in comparison with that in the ligand. When the thioamide group is effectively conjugated to the azulene unit, the deviation of charge distribution may occur through the azulene unit to the thioamide unit because of a stable aromatic cycloheptatrienyl cation (**F** and **G** in Scheme 3). According to the results of our NMR study, the coordination is likely to enhance the conjugation between the

thioamide and azulene moiety, which weaken the C=N double-bond character.

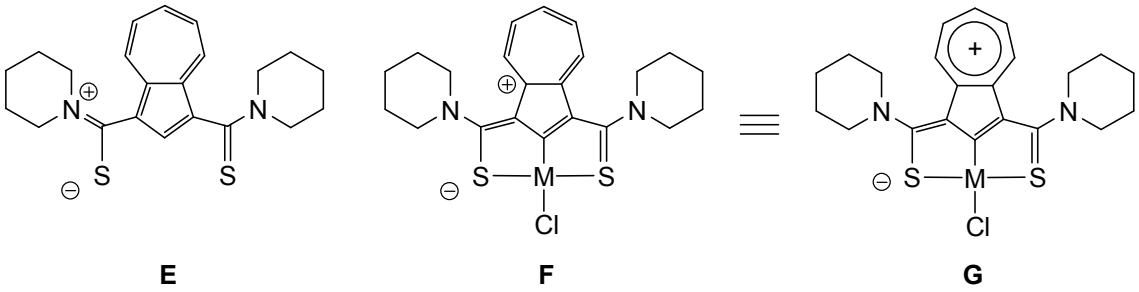

E **F** **G**

Scheme 3. Proposed charge distribution of the thioamide group in the ligand and the pincer complex.

Crystal structures

The solid-state structures of **1-3** were determined by X-ray diffractional studies. Dark blue single crystals of **1** suitable for X-ray diffraction study were obtained by the slow diffusion of hexane into its solution in CH_2Cl_2. In the solid state, ligand **1** has a crystallographic mirror plane (Figure 1a). Single crystals of **2** and **3** were obtained by recrystallization from DMF/ethanol. Complexes **2** and **3** crystallize in the monoclinic space group $P2_1/n$ with a solvating DMF molecule (Figures 1b and 1c). Each metal center has a distorted square-planar geometry.

Figure 1

Table 1 shows selected bond distances and angles of **1-3**. From the comparison of ligand **1** and the complexes, it can be seen that the S=C bond length significantly increases (0.055 - 0.075 Å) upon coordination to the metal center. In contrast, the coordination shortens the C2-C7 and C6-C13 bonds by 0.036 Å in Pd complex **2** and by 0.038 Å in Pt complex **3** on average compared with those in ligand **1**, which are more significant than the shortens of N1-C7 and N2-C13 bonds (0.017 Å for **2** and 0.015 Å for **3**). The significantly shortened C2-C7 and C6-C13 bonds in the complexes are consistent with the result from the NMR study indicating the structure of **G** in Scheme 3 rather than a structure with a C=N double-bond character such as **E**. Since the shortening of the

C2-C7 and C6-C13 bonds was not significant (0.014 Å)[3b] in reference complex **4**, this structural form of **G** is a characteristic of the azulene central ligand. The sulfur atoms in the azulene complexes lie in almost the same plane of the azulene unit, which is confirmed by the small torsion angles of S1-C7-C2-C1 in **2** (15.7°) and **3** (12.4°). The coplanar structure indicates effective conjugation between the thioamide moieties and the azulene unit. The effective conjugation is likely to enhance the delocalization of the positive charge to the central azulene unit and weaken the C=N double-bond contribution. In contrast, ligand **1** has a large torsion angle of S1-C7-C2-C1 (70.1°), indicating ineffective conjugation and localization of the charge on the nitrogen atom.

Table 1

Figure 2

To discuss the effect of the central azulene unit, the crystal structure of Pd complex **2** was compared with those of SCS-pincer complex **4** and SNS-pincer complex **5**. Selected bond lengths and angles of **4** and **5** are also shown in Table 1. In terms of the bond length between the Pd center and the cyclometallating atoms, C1 and N3, azulene complex **2** (1.918 Å) and pyrrole complex **5** (1.938 Å) have shorter M-C or M-N bond, respectively, than the benzene complex **4** (1.961 Å) (Figure 2). The bond length mainly depends on the structure of the central unit, which is five-membered ring or six-menbered ring. The ideal angle of a substituent on a five-membered ring is 126°, which is larger than that of a six-membered ring (120°). In fact, the angle of C1-C2-C7 in ligand **1** is 125.9°. The large angle induces steric strain on the metallacycles and pulls the metal center close to the central unit. This steric strain on the metallacycle is expected to be the origin of the short Pd-C bond in azulene complex **2**. The steric strain on **2** is also confirmed by the small S1-Pd-S2 angle (166.0°) compared with that in **4** (170.8°). Recently, Bourissou *et al.* reported a pincer Pd complex bearing a 2-indenylidene unit with thiophosphonyl sidearms.[15] Although the 2-indenylidene unit has a five-membered ring, the Pd-C bond is relatively long (1.984 Å), presumably due

to the long S=P bond in the thiophosphonyl sidearm, which reduces the steric strain. On the other hand, the Pd-Cl bond length should depend on the electron-donating effect of the cyclometallating atom at the *trans* position, the so-called *trans* influence.[16] Since complexes **2** and **4** have longer Pd-Cl bonds (2.3957 and 2.3973 Å) than complex **5** (2.3159 Å), the cyclometallating carbon atom has a stronger donating property than the nitrogen atom.

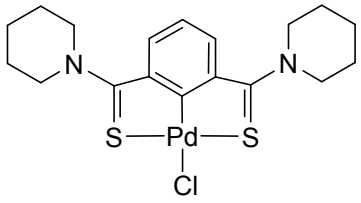

4

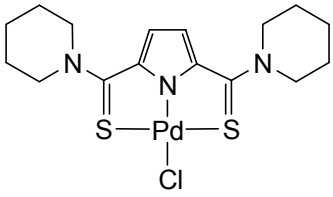

5

UV/Vis spectroscopy

Ligand **1** displays an intense absorption band at 295 nm (ε = 43800 L mol^{-1}cm^{-1}), which can be assigned to the π-π* transition of the azulene moiety (Figure 3a).[17] The absorption spectra of complexes **2** and **3** exhibit a bathochromic shift of the intense absorption to 350 and 353 nm, respectively. The bathochromic shift of the π-π* transition is presumably due to the effective conjugation between the azulene and the thioamide moiety by the metallation, which is observed in the crystal structures. In addition to the π-π* absorption, Pd complex **2** exhibits weak absorption at 480 nm and broad absorption up to 600 nm. The spectrum of Pt complex **3** exhibits broad absorption up to 650 nm. The absorbances in the long-wavelength region were assigned on the bases of DFT calculations (see below). Figure 4 shows the absorption spectra of Pd complexes **2**, **4** and **5** in order to compare the effect of the central structure on absorption. Owing to the central benzene and pyrrole structures of **4** and **5**, the absorption of the π-π* transition is weaker than that of the azulene complex. The

absorptions of complexes **4** and **5** reach 500 and 450 nm, respectively, which are shorter wavelengths than that for complex **2**. The effect of the central structure on the absorption spectrum was also investigated by performing DFT calculations.

Figure 3

Figure 4

DFT calculations

To better understand the UV/Vis absorption spectra in solution, compounds **1**-**5** were examined by theoretical calculations. After optimization of the geometrical structures, time-dependent density functional theory (TD-DFT) calculations were performed at the B3LYP level for **1** and at the B3PW91 level for **2**-**5** with the LANL2DZ basis set implemented in the Gaussian 03 program suite.[18-19] Figure 3b exhibits the calculated UV/Vis spectra of **1**-**3**, which were obtained by the TD-DFT calculations. The calculated spectra of the complexes are in good agreement with the measured spectra shown in Figure 3a. Table 2 shows the main electronic singlet-singlet vertical excitations, their oscillator strengths and their corresponding assignments. Figure 5 shows contour plots for the molecular orbitals of **1**-**3**, which are related to significant transitions with large oscillator strengths (f>0.01) in the low-lying electronic transitions. The results show that the HOMO, LUMO and LUMO + 1 of **1** are localized on the azulene unit and sulfur atoms with π character. The HOMO – 2 of **1** is localized on the azulene unit with a significant contribution of the lone pair of electrons on the sulfur atom. On the basis of the calculation, a ππ* transition (HOMO to LUMO + 1) and nπ* transition (HOMO – 2 to LUMO) were observed at 465 and 457 nm, respectively (Table 2). The calculated absorption at about 460 nm accounts for these two transitions, which is probably related to the absorption at 415 nm in the measured spectrum (Figure 3). The HOMO – 1 of Pd complex **2** is mainly localized on the d orbital of the Pd metal, while the LUMO and LUMO + 2 are basically composed of the π orbital of the pincer ligand. The calculated excitation at 609 nm corresponds to the transition from the metal

center (HOMO – 1) to the π* orbital on the azulene moiety (LUMO), which can be categorized as metal-to-ligand charge transfer (MLCT) (Figure 5b). The MLCT absorption is the origin of the broad absorption reaching 600 nm in the measured spectra (Figure 3a). The other MLCT from HOMO – 1 to the π* orbital on the thioamide moiety (LUMO + 2) is attributed to the absorption at 480 nm. The HOMO – 1 and HOMO – 2 of Pt complex **3** are localized on the d orbital of the Pt center and partly on the π orbital of the ligand. The LUMO of **3** is delocalized exclusively on the expanded π orbital of the pincer ligand. In contrast to Pd complex **2**, Pt complex **3** has three strong theoretical transitions at 600, 524 and 448 nm. The lowest transition at 600 nm is associated with MLCT, which is mainly composed of the transition from HOMO -1 to LUMO (Figure 5c). The other transitions are composed of a mixture of MLCT and a ππ* transition. These close-lying transitions are likely to be the origin of the broad absorption from 450 nm to 650 nm in the measured spectrum of **3**. TD-DFT calculations also provided information on the electronic transitions of the reference complexes **4** and **5**. According to the lowest electronic transition energy with large oscillator strength (f>0.01), complexes **4** and **5** have larger transition energies (2.11 and 2.23 eV, respectively) than azulene complex **2** (2.04 eV). This tendency is in agreement with the wavelength of the absorption edge shown in Figure 4. The lowest-energy transition of **4** is assigned to the transition from the Pd center (HOMO – 1) to the π* orbital on the central aromatic unit (LUMO), which is similar to the lowest-energy transition of the azulene complex. Since the energy levels of HOMO – 1 in **2** and **4** are essentially the same (-5.29 and -5.32 eV, respectively), the difference in the lowest transition energy is attributed to their LUMO levels (-2.83 and -2.64 eV, respectively). Since their LUMO are composed of π* orbitals on each central unit such as azulene and benzene, the low LUMO level of azulene complex **2** is due to the extended π electron system of the azulene unit. Therefore, the azulene complex has an MLCT band in a longer-wavelength region compared with the reference complexes.

Conclusion

SCS-pincer complexes with an azulene unit were synthesized and characterized by X-ray crystallography. Their structural and optical properties were discussed in comparison with those of related complexes with a benzene and pyrrole unit. The unique structure of the azulene unit affects the electron density of the thioamide moiety in the complex; the positive charge on the nitrogen atom is delocalized in the azulene unit to form an aromatic cycloheptatrienyl cation. DFT calculations for the azulene complexes revealed that the origin of the long-wavelength absorption is a transition from the metal center to the extended π system of the azulene unit.

Experimental

General, measurement, and materials. ^{1}H-NMR spectra were recorded on a JEOL Lambda-300 and a JEOL EX-270 NMR spectrometer. IR spectra were recorded on a JASCO IR-810 spectrophotometer. UV/Vis spectra were measured with a Shimadzu UV-2550 and UV-3100PC UV-visible spectrophotometer. Mass spectrum was recorded on a JEOL JMS-700 MStation using *m*-nitrobenzyl alcohol as a matrix. Elemental analyses were carried out with a Yanaco MT-5 CHN autorecorder. Azulene, $PdCl_2$, $[PtCl_2(PhCN)_2]$ and other chemicals were used as received from commercial suppliers. Anhydrous THF and DMF were purchased from Kanto Chemical and used as a dry solvent. 1,3-Bis(piperidinocarbonyl)azulene[12] and Pd complex **4**[3b] were prepared according to the literature methods.

1,3-Bis(piperidinothiocarbonyl)azulene (1).

A mixture of 1,3-Bis(piperidinocarbonyl)azulene (90 mg, 0.22 mmol) and Lawesson's reagent (177 mg, 0.44 mmol) in anhydrous THF (5 mL) was heated under reflux for 15 h in a nitrogen atmosphere. After cooling to room temperature, the product

was isolated by column chromatography on silica-gel using $CHCl_3$ as an eluent (111 mg, 84%). Crystal of **1** suitable for the X-ray diffraction study was obtained by recrystallization from CH_2Cl_2/hexane. ^{1}H NMR (300 MHz, $CDCl_3$): δ 8.57 (2H, d, *J* = 9.7 Hz), 7.74 (1H, s), 7.69 (1H, t, *J* = 9.9 Hz), 7.32 (1H, t, *J* = 9.9 Hz), 4.47 (4H, br), 2.78 (4H, br), 1.88-1.30 (12H, m). ^{13}C{^{1}H} (75 MHz, $CDCl_3$): δ 194.0, 139.9, 137.3, 136.1, 133.3, 129.4, 125.7, 53.8, 50.7, 27.4, 25.8, 24.3. FT-IR (KBr, cm^{-1}) 3003, 2935, 2853, 1591, 1573, 1480, 1440, 1413, 1367, 1237, 1132, 1022, 1006, 746. Anal. calcd for $C_{22}H_{26}N_2S_2 \cdot CH_2Cl_2$: C 59.09, H 6.04, N 5.99; found C 59.42, H 6.26, N, 5.97.

Chloro[2,6-bis(piperidinothiocarbonyl-κ*S*)azulenyl-κ*C*^{1}]palladium(II) (2).

To a solution of $PdCl_2$ (11 mg, 0.062 mmol) and LiCl (5.3 mg, 0.13 mmol) in MeOH (2 mL) was added ligand **1** (30 mg, 0.078 mmol). The mixture was heated under reflux for 18 h in a nitrogen atmosphere. After cooling to room temperature, the precipitate was collected by filtration and washed with MeOH (25 mg, 77%). Crystal of **2**·DMF suitable for the X-ray diffraction study was obtained by recrystallization from DMF/EtOH. ^{1}H NMR (270 MHz, DMSO): δ 8.24 (2H, d, *J* = 10.0 Hz), 7.99 (1H, t, *J* = 9.7 Hz), 7.79 (2H, t, *J* = 9.9 Hz), 4.13 (8H, br), 1.76 (12H, s). FT-IR (KBr, cm^{-1}) 2929, 1515, 1455, 1388, 1240, 1011, 864, 744. HRMS(FAB): 487.0528 (Calcd. for $[M\text{-}Cl]^+$: 487.0501). Anal. calcd for $C_{22}H_{25}N_2ClPdS_2 \cdot 0.5H_2O$: C 49.63, H 4.92, N 5.26; found C 49.88, H 4.65, N, 5.25.

Chloro[2,6-bis(piperidinothiocarbonyl-κ*S*)azulenyl-κ*C*^{1}]platinum(II) (3).

To a solution of $PtCl_2(PhCN)_2$ (16 mg, 0.031 mmol) in $CHCl_3$ (1 mL) was added ligand **1** (17 mg, 0.043 mmol) in acetonitrile (3mL). The mixture was stirred at 65 °C for 18 h in a nitrogen atmosphere. After cooling to room temperature, the precipitate was collected by filtration and washed with MeOH (22 mg, 85%). Crystal of **3**·DMF suitable for the X-ray diffraction study was obtained by recrystallization from

DMF/EtOH. ^{1}H NMR (270 MHz, DMSO): δ 8.28 (2H, d, *J* = 9.0 Hz), 8.07 (1H, t, *J* = 9.6 Hz), 7.68 (2H, t, *J* = 9.9 Hz), 4.14(8H, br), 1.78 (12H, s). FT-IR (KBr, cm^{-1}) 2933, 1521, 1427, 1238, 1009, 827, 760, 482. HRMS(FAB): 576.1141 (Calcd. for $[M-Cl]^{+}$: 576.1109). Anal. calcd for $C_{22}H_{25}N_2ClPtS_2 \cdot 0.5H_2O$: C 42.54, H 4.22, N 4.51, Cl 5.71, S 10.32; found C 42.34, H 3.94, N 4.69, Cl 5.68, S 10.02.

1,3-Bis(piperidinothiocarbonyl)pyrrole.

To a mixture of sulfur (S_8) (65 mg, 2.0 mmol) and piperidine (0.24 mL, 2.4 mmol) in anhydrous DMF (4 mL) was added pyrrole-2,5-dicarbaldehyde (100 mg, 0.81 mmol). The mixture was stirred at 115 °C for 20 h in a nitrogen atmosphere. After cooling to room temperature, an aqueous solution of NH_4Cl was added. The organic material was extracted with $CHCl_3$. The product was isolated by column chromatography on silica-gel using $CHCl_3$ as an eluent (194 mg, 74%). ^{1}H NMR (270 MHz, $CDCl_3$): δ 10.1 (1H, br), 6.28 (2H, s), 4.15 (8H, br), 1.56-1.25(12H, m). $^{13}C\{^{1}H\}$ (75 MHz, $CDCl_3$): δ 186.5, 133.1, 109.7, 53.1, 26.4, 24.5. FT-IR (KBr, cm^{-1}) 3364, 2936, 2851, 1524, 1508, 1487, 1439, 1260, 1241, 1005, 784. MS(FAB): 322 (Calcd. for $[M]^{+}$: 322). Anal. calcd for $C_{16}H_{23}N_3S_2$: C 59.77, H 7.21, N 13.07 ; Found C 59.66, H 7.02, N 13.01.

Chloro[2,6-bis(piperidinothiocarbonyl-κ*S*)pyrrole-κ*N*]palladium (5).

To a solution of $PdCl_2$ (12 mg, 0.068 mmol) and LiCl (5.9 mg, 0.14 mmol) in MeOH (3 mL) was added 1,3-bis(piperidinothiocarbonyl)pyrrole (20 mg, 0.062 mmol). The mixture was heated under reflux for 10 h in a nitrogen atmosphere. After cooling to room temperature, the precipitate was collected by filtration and washed with MeOH (21 mg, 73%). Crystal of **5** suitable for the X-ray diffraction study was obtained by recrystallization from $CHCl_3$/hexane. ^{1}H NMR (270 MHz, $CDCl_3$): δ 6.37 (2H, s), 4.19 (4H, br), 3.99 (4H, br), 1.78(12H, br). $^{13}C\{^{1}H\}$ NMR (100 MHz, $CDCl_3$): δ 187.1, 142.7, 115.7, 53.7, 26.4, 25.7, 23.4. FT-IR (KBr, cm^{-1}) 2934, 2852, 1537, 1265,

1244, 1017. MS(FAB): 426 (Calcd. for $[M\text{-}Cl]^+$: 426). Anal. calcd for $C_{16}H_{22}ClN_3PdS_2$: C 41.56, H 4.80, N 9.09, Cl 7.67, S 13.87; found C 41.31, H 4.60, N 9.13, Cl 7.74, S 13.66.

Computational Details.

The geometrical structures were optimized at the B3LYP for **1** and the B3PW91 level for **2**-**5** with LANL2DZ basis set implemented in Gaussian 03 program suite.[18-19] Using the optimized geometries of **1**-**3**, TD-DFT calculations were performed at the B3LYP for **1** and the B3PW91 level for **2**-**5** to predict their absorptions.

Crystal structure determination.

Crystals of **1**, **2**, **3** and **5** for X-ray analysis were obtained as described in the preparations. Intensity data were collected on a Rigaku R-AXIS Rapid diffractometer with Mo *K*α radiation. Crystals were mounted on glass capillary tubes. Crystallographic data and details of refinement of the complexes are summarized in Table 3. A full matrix least-squares refinement was used for non-hydrogen atoms with anisotropic thermal parameters method by SHELXL-97 program. Hydrogen atoms were placed at the calculated positions and were included in the structure calculation without further refinement of the parameters. CCDC 750102, 750103, 750104 and 750105 contains the supplementary crystallographic data for compounds **1**, **2**, **3** and **5**, respectively. These data can be obtained free of charge via http://www.ccdc.cam.ac.uk/conts/retrieving.html, or from the Cambridge Crystallographic Data Centre, 12 Union Road, Cambridge CB2 1EZ, UK; fax: (+44) 1223-336-033; or e-mail: deposit@ccdc.cam.ac.uk.

Acknowledgement

This work was partly supported by Grant-in-Aid for Young Scientists (Start-up) (20850003) and Grant-in-Aid for Scientific Research (C) (20550105). The authors are

grateful to the Chemical Analysis Center of University of Tsukuba for X-ray diffractional studies, elemental analyses and NMR spectroscopy. The authors wish to thank to Dr. Jun-Chul Choi and Dr. Yasumasa Takenaka for the measurement and refinement of the crystal structure.

References

[1] (a) M. Albrecht and G. van Koten, *Angew. Chem., Int. Ed.*, 2001, **40**, 3750; (b) J. T. Singleton, *Tetrahedron*, 2003, **59**, 1837; (c) M. E. van der Boom and D. Milstein, *Chem. Rev.*, 2003, **103**, 1759; (d) D. Pugh and A. A. Danopoulos, *Coord. Chem. Rev.*, 2007, **251**, 610; (e) S. J. Farley, D. L. Rochester, A. L. Thompson, J. A. K. Howard and J. A. G. Williams, *Inorg. Chem.,* 2005, **44**, 9690; (f) J. Ito, S. Ujiie and H. Nishiyama, *Organometallics*, 2009, **28**, 630.; (g) M. Ashizawa, L Yang, K. Kobayashi, H. Sato, A. Yamagishi, F. Okuda, T. Harada, R. Kuroda and M. Haga, *Dalton Trans.*, 2009, 1700; (h) C. A. Kruithof, A. Berger, H. P. Dijkstra, F. Soulimani, T. Visser, M. Lutz, A. L. Spek, R. J. M. K. Gebbink and G. van Koten, *Dalton Trans.*, 2009, 3306; (i) S. Stoccoro, G. Alesso, M. A. Cinellu, G. Minghetti, A. Zucca, M. Manassero and C. Manassero *Dalton Trans.*, 2009, 3467.

[2] For the first example of a thioamide pincer complex; S. Takahashi, M. Nonoyama and M. Kita, *Transition Met. Chem*., 1995, **20**, 528.

[3] (a) T. Kanbara, K. Okada, T. Yamamoto, H. Ogawa and T. Inoue, *J. Organomet. Chem.,* 2004, **689**, 1860; (b) M. Akaiwa, T. Kanbara, H. Fukumoto and T, Yamamoto, *J. Organomet. Chem,*. 2005, **690**, 4192; (c) K. Okamoto, T. Kanbara, T. Yamamoto and A. Wada, *Organometallics,* 2006, **25**, 4026; (d) K. Okamoto, T. Yamamoto, M. Akita, A. Wada and T. Kanbara, *Organometallics,* 2009, **28**, 3307; (e) J. Kuwabara and T. Kanbara, *J. Photopolym. Sci. Technol.*, 2008, **21**, 349.

[4] (a) M. A. Hossain, S. Lucarini, D. Powell and K. Bowman-James *Inorg. Chem.,* 2004, **43**, 7275; (b) R. A. Begum, D. Powell and K. Bowman-James, *Inorg. Chem.,* 2006, **45**, 964; (c) V. A. Kozlov, D. V. Aleksanyan, Yu. V. Nelyubina, K. A. Lyssenko, E. I. Gutsul, L. N. Puntus, A. A. Vasil'ev, P. V. Petrovskii and I. L. Odinets, *Organometallics,* 2008, **27**, 4062.

[5] K. Okamoto, T. Kanbara and T. Yamamoto, *Chem. Lett.,* 2006, **35**, 558.

[6] C. Mazet and L. H. Gade, *Chem. Eur. J.,* 2002, **8**, 4308.

[7] (a) C. Lambert, G. Nöll, M. Zabel, F. Hampel, E. Schmälzlin, C. Bräuchle and K. Meerholz, *Chem. Eur. J.,* 2003, **9**, 4232; (b) L. Cristian, I. Sasaki, P. G. Lacroix, B. Donnadieu, I. Asselberghs, K. Clays and A. C. Razus, *Chem. Mater.,* 2004, **16**, 3543; (c) J. Zhang and S. Petoud, *Chem. Eur. J.,* 2008, **14**, 1264.

[8] (a) F. Wang, Y. Lai and M. Han, *Macromolecules*, 2004, **37**, 3222; (b) X. Wang, J. K. Ng, P. Jia, T, Lin, C. M. Cho, J. Xu, X. Lu and C. He, *Macromolecules*, 2009, **42**, 5534.

[9] (a) T. Zieliński, M. Kędziorek and J. Jurczak, *Tetrahedoron Lett.*, 2005, **46**, 6231; (b) T. Zieliński, M. Kędziorek and J. Jurczak, *Chem. Eur. J.,* 2008, **14**, 838; (c) S. Wakabayashi, Y. Kato, K. Mochizuki, R. Suzuki, M. Matsumoto, Y. Sugihara and M. Shimizu, *J. Org. Chem.,* 2007, **72**, 744.

[10] (a) J. J. Schneider, D. Wolf, C. Janiak, O. Heinemann, J. Rust and C. Krüger, *Chem. Eur. J.,* 1998, **4**, 1982; (b) S. Aime, A. J. Arce, D. Giusti, R. Gobetto and J. W. Steed, *J. Chem. Soc., Dalton Trans.*, 2000, 2215; (c) K. Matsubara, T. Oda and H. Nagashima, *Organometallics*, 2001, **20**, 881; (d) K. Tsuchiya, K. Ideta, K. Mogi, Y. Sunada and H. Nagashima, *Dalton Trans.*, 2008, 2708; (e) J, A, Cabeza, I. del Río, J. M. Fernández-Colinas, P. García-Álvarez and D. Miguel, *Organometallics*, 2007, **26**, 1414.

[11] (a) S. R. Graham, G. M. Ferrence and T. D. Lash, *Chem. Commun*., 2002, 894; (b) D. Liu and T. D. Lash, *Chem. Commun*., 2002, 2426; (c) T. D. Lash, D. A. Colby, S. R. Graham, G. M. Ferrence and L. F. Szczepura, *Inorg. Chem.,* 2003, **42**, 7326.

[12] V. A. Nefedov and L. K. Tarygina, *Zh. Org. Khim.* 1994, **30**, 1639.

[13] (a) D. R. M. de Moreira, *Synlett*, 2008, 463; (b) M. Jesberger, T. P. Davis and L. Barner, *Synthesis*, 2003, 1929.

[14] K. B. Wiberg and P. R. Rablen, *J. Am. Chem. Soc.*, 1995, **117**, 2201.

[15] P. Oulié, N. Nebra, N. Saffon, L. Maron, B. Martin-Vaca and D. Bourissou, *J. Am. Chem. Soc.*, 2009, **131**, 3493.

[16] T. G. Appleton, H. C. Clark and L. E. Manzer, *Coord. Chem. Rev.,* 1973, **10**, 335.

[17] (a) P. Foggi, F. V. R. Neuwahl, L. Moroni and P. R. Salvi, *J. Phys. Chem. A*, 2003, **107**, 1689; (b) S. V. Shevyakov, H. Li, R. Muthyala, A. E. Asato, J. C. Croney, D. M. Jameson and R. S. H. Liu, *J. Phys. Chem. A*, 2003, **107**, 3295.

[18] (a) M. J. Frisch, G. W. Trucks, H. B. Schlegel, G. E. Scuseria, M. A. Robb, J. R. Cheeseman, J. A. Montgomery Jr., T. Vreven, K. N. Kudin, J. C. Burant, J. M. Millam, S. S. Iyengar, J. Tomasi, V. Barone, B. Mennucci, M. Cossi, G. Scalmani, N. Rega, G. A. Petersson, H. Nakatsuji, M. Hada, M. Ehara, K. Toyota, R. Fukuda, J. Hasegawa, M. Ishida, T. Nakajima, Y. Honda, O. Kitao, H. Nakai, M. Klene, X. Li, J. E. Knox, H. P. Hratchian, J. B. Cross, V. Bakken, C. Adamo, J. Jaramillo, R. Gomperts, R. E. Stratmann, O. Yazyev, A. J. Austin, R. Cammi, C. Pomelli, J. W. Ochterski, P. Y. Ayala, K. Morokuma, G. A. Voth, P. Salvador, J. J. Dannenberg, V. G. Zakrzewski, S. Dapprich, A. D. Daniels, M. C. Strain, O. Farkas, D. K. Malick, A. D. Rabuck, K. Raghavachari, J. B. Foresman, J. V. Ortiz, Q. Cui, A. G. Baboul, S. Clifford, J. Cioslowski, B. B. Stefanov, G. Liu, A. Liashenko, P. Piskorz, I. Komaromi, R. L. Martin, D. J. Fox, T. Keith, M. A. Al-Laham, C. Y. Peng, A. Nanayakkara, M. Challacombe, P. M. W. Gill, B. Johnson, W. Chen, M. W. Wong, C. Gonzalez and J. A. Pople, Gaussian 03, Revision D.01, Gaussian, Inc., Wallingford CT, 2004; (b) J. P. Foster and F. Winhold, *J. Am. Chem. Soc.,* 1980, **102**, 7211; (c) E. D. Glendening, A. E. Reed, J. E. Carpenter and F. Weinhold, NBO Version 3.1.

[19] GaussView, Version 4.1, Roy Dennington II, Todd Keith and John Millam, Semichem, Inc., Shawnee Mission, KS, 2007.

Table 1.
Selected Bond Distance (Å) and Angle (deg) for Compound **1-5**

	1	**2**	**3**	**4**[c]	**5**
M-C1		1.918(2)	1.910(3)	1.961(2)	1.938(2)[a]
M-S1		2.3128(6)	2.3056(9)	2.2939(5)	2.298(3)[b]
M-S2		2.3374(6)	2.311(1)	2.2984(4)	2.310(2)[b]
M-Cl1		2.3957(6)	2.408(1)	2.3973(5)	2.3159(6)
S1-C7	1.680(2)	1.752(2)	1.743(3)	1.720(2)	1.740(3) [b]
S2-C13		1.735(2)	1.755(4)	1.723(2)	1.741(3) [b]
C2-C7	1.487(4)	1.455(3)	1.449(5)	1.487(2)	1.460(4)
C6-C13		1.448(3)	1.450(5)	1.480(2)	1.457(4)
N1-C7	1.343(3)	1.321(3)	1.336(5)	1.324(2)	1.363(3)
N2-C13		1.332(3)	1.320(5)	1.327(2)	1.357(3)
C1-M-S1		96.81(2)	97.19(3)	96.18(2)	95.93(6)[a,b]
C1-M-S2		96.73(2)	95.90(3)	92.97(2)	96.32(5)[a,b]
Cl1-M-C1		178.97(7)	178.6(1)	176.83(5)	179.56(5)[a]
S1-M-S2		165.96(2)	166.91(3)	170.84(2)	167.81(7)[b]
S1-M-C1		82.68(7)	83.0(1)	85.52(5)	83.70(9)[a,b]
S2-M-C1		83.71(7)	83.9(1)	85.33(5)	84.04(9)[a,b]

[a] C1 indicates N3 in complex **5**, [b] The average length and angle of disordered atoms.
[c] From reference 3b.

Table 2. Main Theoretical Electronic Transitions, with Composition, Corresponding Oscillator Strength (*f*) and Assignment

Compound	Calcd Transition(nm)	Composition [a]	f [b]	Assignment
1	465	H → L + 1 (56%)	0.0429	ππ*
	457	H – 2 → L (58%)	0.0262	nπ*
2	609	H – 1 → L (67%)	0.0118	MLCT
	487	H – 1 → L + 2 (43%)	0.0623	MLCT
3	600	H – 1 → L (63%)	0.0168	MLCT
	524	H – 2 → L (50%)	0.0393	MLCT/ππ*
	448	H – 1→ L + 2 (58%)	0.0775	MLCT/ππ*
4	589	H – 1 → L (69%)	0.0137	MLCT
5	556	H → L (57%)	0.0135	MLCT

[a] H denotes HOMO and L denotes LUMO. [b] Oscillator strengths.

Table 3.
Crystal Data and Details of Structure Refinement of Complexes **1**, **2**, **3** and **5**

	1	**2**	**3**	**5**
Chemical formula	$C_{22}H_{26}N_2S_2 \cdot CH_2Cl_2$	$C_{22}H_{25}N_2ClS_2Pd \cdot C_3H_7NO$	$C_{22}H_{25}N_2ClS_2Pt \cdot C_3H_7NO$	$C_{16}H_{22}N_3ClPdS_2$
Formula weight	467.51	596.52	685.21	462.34
Crystal system	orthorhombic	monoclinic	monoclinic	triclinic
Space group	Pnma (No. 62)	$P2_1/n$ (No. 14)	$P2_1/n$ (No. 14)	P-1 (No 2)
a, Å	16.1348(6)	12.7161(6)	11.6349(3)	9.4925(5)
b, Å	16.0405(7)	14.7195(5)	15.3558(4)	10.1758(4)
c, Å	8.8982(3)	13.6311(6)	13.7152(3)	10.9510(4)
α, deg				61.6480(10)
β, deg		91.4037(14)	96.3359(8)	73.5321(17)
γ, deg				85.2855(17)
V, Å^3	2302.95(15)	2550.64(19)	2435.44(10)	891.00(6)
Z	4	4	4	2
μ, cm^{-1}	4.757	10.198	60.440	14.278
F(000)	984	1224	1352	468
D_{calcd}, g cm^{-3}	1.348	1.553	1.869	1.723
Crystal size, mm	0.30x0.15x0.15	0.20x0.10x0.10	0.25x0.20x0.20	0.30x0.30x0.20
Exposure rate sec. / °	60.0	150.0	60.0	20.0
No. of date	20625	23767	23350	8856
No. of unique date	2713	5793	5525	4033
No. of variables	144	299	282	207
R ($I > 2\sigma(I)$)	0.0501	0.0317	0.0279	0.0213
R (All reflections)	0.0884	0.0436	0.0329	0.0282
R_W *(All reflections)*	0.1578	0.0705	0.0631	0.0548
GOF	1.183	1.085	1.074	1.162

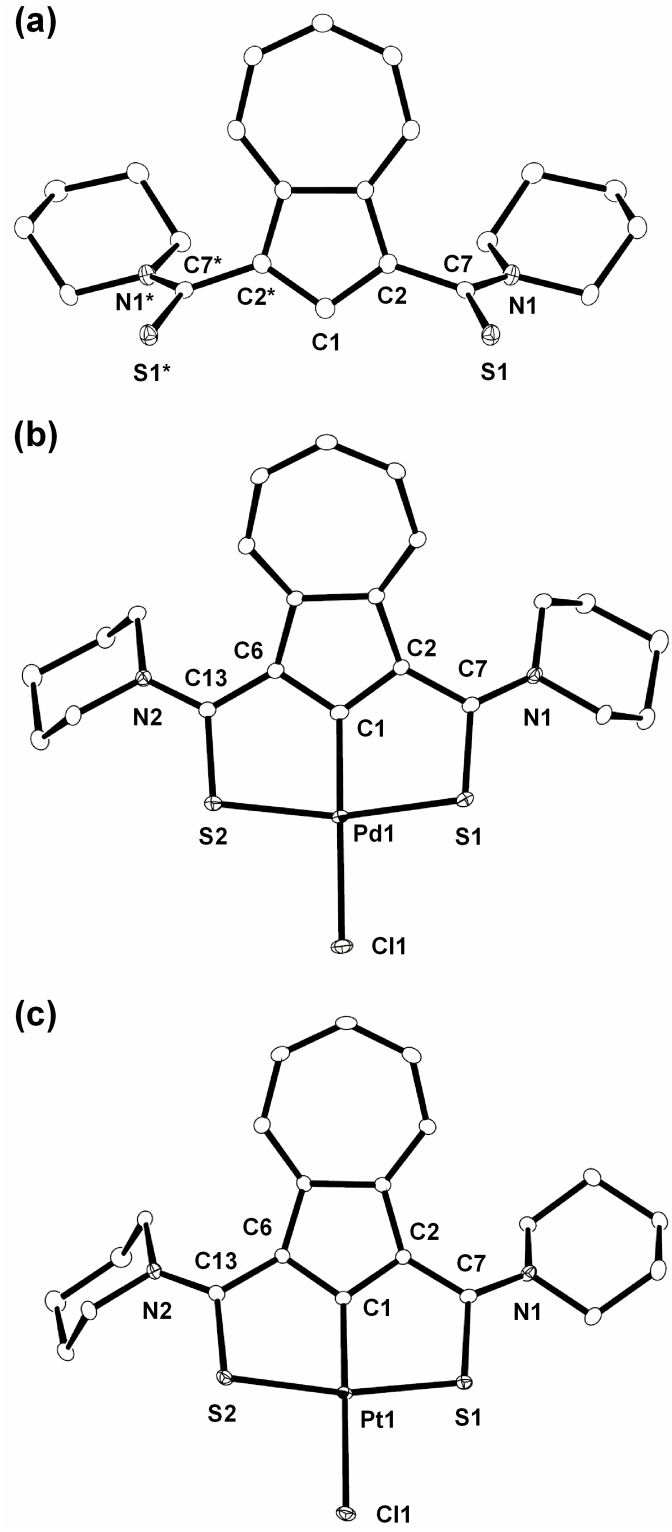

Figure 1. ORTEP drawing of (a) **1,** (b) **2** and (c) **3** with thermal ellipsoids shown at the 30% probability level. Hydrogen atoms and solvating molecules are omitted for clarity. Atoms with asterisks are crystallographically equivalent to those having the same number without asterisks.

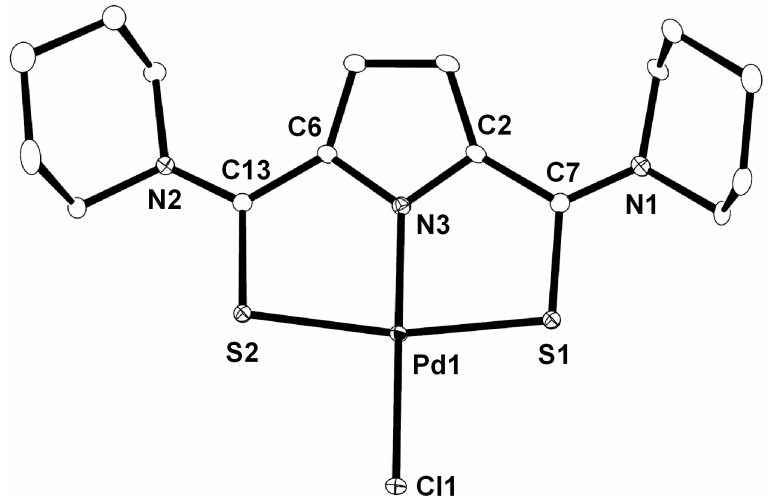

Figure 2. ORTEP drawing of **5** with thermal ellipsoids shown at the 30% probability level. Hydrogen atoms are omitted for clarity. S1 and S2 atoms show one of the disordered positions.

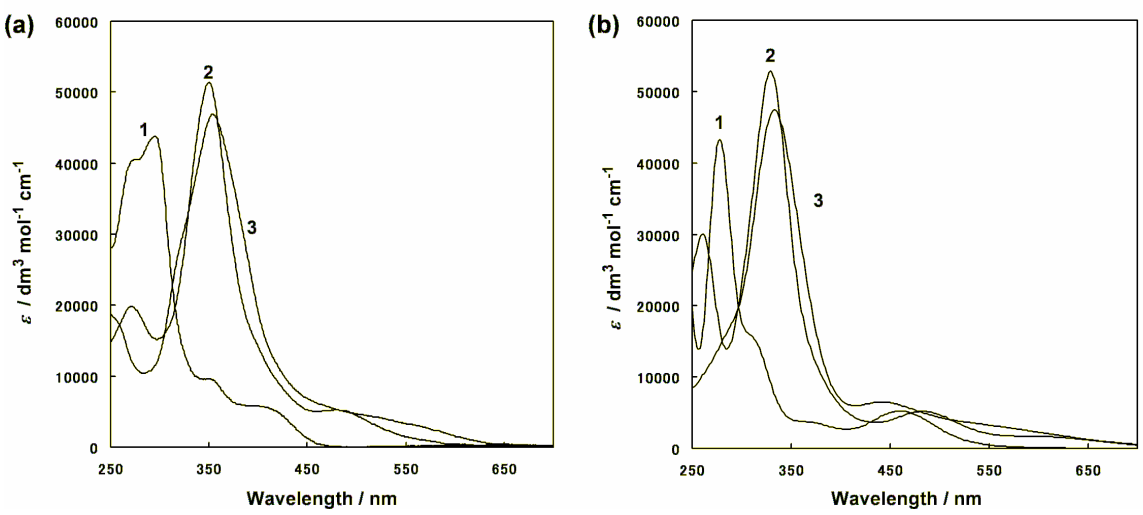

Figure 3. (a) UV/Vis spectra in CH_2Cl_2 (b) Calculated UV/Vis spectra of **1**, **2** and **3**.

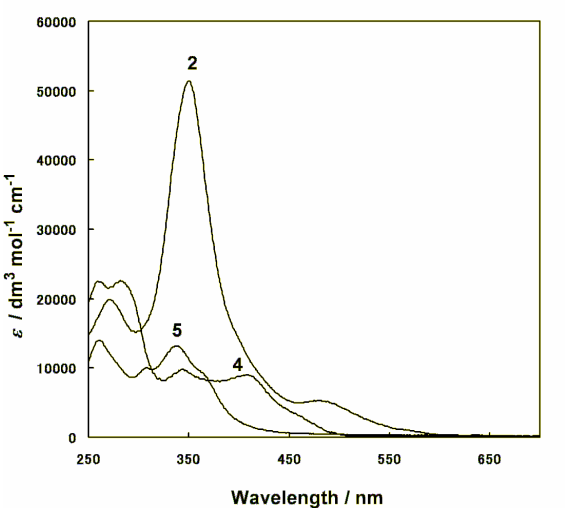

Figure 4. UV/Vis spectra of **2**, **4** and **5** in CH_2Cl_2.

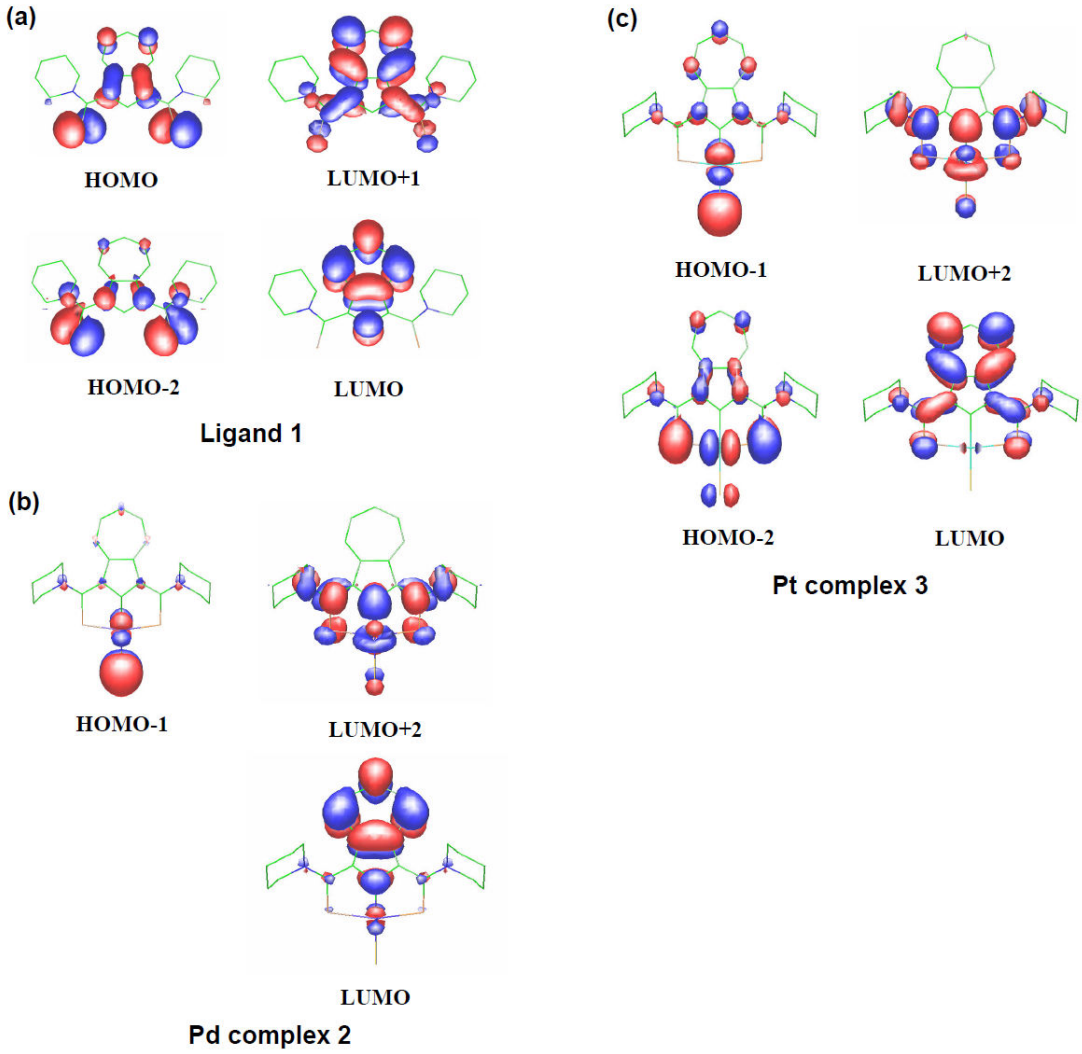

Figure 5. Contour plots of (a) ligand **1**, (b) Pd complex **2** and (c) Pt complex **3**.